

# Evaluating the Effect of Land Cover, Seasonality and Delineation Method on Runoff at the Watershed Scale

Katherine Clancy

College of Natural Resources, University of Wisconsin-Stevens Point, Stevens Point, WI, USA  
Email: kclancy@uwsp.edu

**How to cite this paper:** Clancy, K. (2021) Evaluating the Effect of Land Cover, Seasonality and Delineation Method on Runoff at the Watershed Scale. *Journal of Water Resource and Protection*, 13, 750-765.  
<https://doi.org/10.4236/jwarp.2021.139039>

**Received:** August 5, 2021

**Accepted:** September 25, 2021

**Published:** September 28, 2021

Copyright © 2021 by author(s) and Scientific Research Publishing Inc. This work is licensed under the Creative Commons Attribution International License (CC BY 4.0).

<http://creativecommons.org/licenses/by/4.0/>



Open Access

---

## Abstract

The aim of this study was to determine if runoff estimates from the curve number model were affected by seasons for different land covers. Eighteen watersheds with varying land covers were delineated using three methods. The delineation methods differ in how internal drainage is evaluated. Runoff estimates from storms for spring, summer, and fall were compared to observed runoff from USGS gaging station data. Errors (difference between estimate runoff and observed runoff) were found to be highest for fall by 3% for all the two delineation methods which do not consider internal drainage. Watersheds were categorized by their dominant land cover (agriculture, forest, or urban). Seasonal differences were found to be significant for certain land covers. The greatest differences between observed and estimated data were found in agriculture and urban especially spring versus fall for all delineations. Forest land cover was found to have no seasonal difference for all three delineation methods. The research suggests that this work contributes to the growing body of research suggesting that vegetative seasonal differences have a greater impact on runoff than is accounted for in the runoff model.

## Keywords

Runoff, Curve Number, Vegetation, Seasonal

---

## 1. Introduction

The ability to accurately model runoff is paramount to watershed and land use management. One of the prevalent models used to estimate runoff is the SCS curve number method (CN method) [1] [2] [3]. The CN method is widely used in part because it has few input conditions and requires knowledge of only two

variables: hydrologic soil type and land cover [4]. It still remains the dominant model in use today both in the US and in many other countries [5] [6]. Despite its limitations, efforts continue to expand its use to other countries. [5] [6] [7]

Most watershed-scale models rely on satellite spatial data to make estimations [8] [9]. A significant source of error is associated with using algorithms to delineate the watershed boundary [10]. Improvements have been made in this regard by refining watershed delineation algorithms especially in regions with low relief, karst topography, substantial internal drainage features (such as wetlands), and/or thick sand layers [11] [12] [13] [14] [15].

One of the most prevalent models for watershed delineation is called the D8 method or standard fill model (SFM) and relies upon elevation differences [8] [9]. This method is part of the toolbox that comes with ArcMap 10.2 Hydrology package and is widely used to delineate watersheds [12] [13] [14] [15]. It assumes that all area included within the watershed contributes to the outlet. The term “standard fill” comes from the tool that fills in any depressions that create internal drainage within the spatial elevation data. This process of filling in these depressions can overestimate runoff where areas within the watershed are not contributing to the outlet [14] [15].

A minor modification to the SFM method is to “cut out” the internal drainage area from the original watershed [13] [15]. Typically, this involves removing wetlands and small depressions found in the watershed. This cut method (CM) does reduce a modest amount of the overestimation, but in areas where wetlands were modified over a century ago, modern spatial land cover satellite data does not capture these features.

A more meticulous approach to watershed delineation is to evaluate the potential contributing source areas (PCSAM) to the outlet. This method uses an algorithm that evaluates the streams, wetlands, and areas adjacent to these features. It also examines the upstream gradient to the outlet where these features are directly connected [11]. A drawback is that this method requires substantially more data and processing time. It also has a bias towards underestimating runoff [13] [14] [15].

A second substantial source of error is associated with assumptions about the land cover data, especially in areas with vegetation [16]. For example, agricultural land covers will have different roughness seasonally. During spring most models including the CN method may underestimate runoff, and during early fall (before harvest) runoff may be overestimated.

Vegetative impacts on surface runoff are reasonably well established in the research literature [16]. Vegetative seasonal change impacts on runoff are less well understood [5] [6] [7] [17]. A growing body of research indicates that vegetative seasonal changes may significantly impact the CN method model. These studies have focused on both shifts in vegetation and the growing season due to climate changes [18] [19].

Gal *et al.* (2017) found that vegetative differences explained over 42% of the

difference between past runoff and present runoff in the Sahel [20]. Geng *et al.* (2020) established that the climatic impacts have extended the growing season, changed the vegetative phenology, and reduced runoff in the Luanhe River Basin in North China [18]. Ji *et al.* (2021) discovered that vegetative change impacted runoff changes by 64% [21]. Similar findings by Hwang *et al.* (2018) indicate that changes in vegetation have affected the surface hydrology and runoff response in forested wetlands in Appalachia [19].

The objective of this paper is to examine how runoff is modeled for different land covers for three different methods of delineation for the spring, summer, and fall seasons. It is a unique study because it includes a large number of watersheds with robust datasets for discharge and precipitation. Using the CN method, the modeled runoff will be compared to observed runoff at a USGS gaging station. A metric called the standard error is used to compare the differences between observed versus modeled runoff. The expectation is that observed seasonal runoff will have the greatest difference in land cover that changes with season (e.g. agricultural) and the least seasonal difference in urban land cover. The SFM and CM are expected to show greater differences in standard error compared to the PCSAM method over the seasons. The significance of this study is to determine if curve number models would be improved with a consideration of season in the curve number coefficient.

## 2. Study Area

Wisconsin has varied geology across the state that includes complex internal drainage and sinks such as wetlands and karst topography [22]. Eighteen watersheds across the state of Wisconsin were selected for this study to include the karst, glaciated, and outwash plains region of the state. Watersheds were selected using three criteria: 1) Stations with 15 years of USGS gaging station daily discharge data [23]; 2) Corresponding NCDC daily precipitation data [24]; 3) A variety of land cover types within the watershed so that no single land type dominated. The watersheds and their locations across the state of Wisconsin are shown in **Figure 1**.

## 3. Methods

The watersheds were delineated using ArcMap 10.2 using three different algorithms and required different spatial data inputs. All methods require a spatial elevation grid called a Digital Elevation Model (DEM). The DEMs in this project are at 10-meter resolution and are a product of the USGS National Elevation Dataset (NED) [25]. The 2011 National Land Cover database was used for land use and land cover [26]. Hydrologic Soil Type was obtained from the US Department of Agriculture [27]. Stream hydrography data was obtained from the Wisconsin Department of Natural Resources [28]. The details of the different algorithms are described in detail in Miller and Clancy (2017) [15]. For convenience, the algorithms will be summarized with the pertinent details related.



**Figure 1.** Location of watersheds based on Miller and Clancy (2017) [15].

### 3.1. Algorithm 1: Standard Fill Method

The standard fill method (SFM) is the algorithm that comes with the ArcMap 10.2 hydrologic package. As with all the algorithms described in this research, the SFM requires the DEM. The DEM is smoothed through a tool called “fill” that removes depressions that could create internal drainage. The process of filling depressions affects the shape and size of the final delineated watershed. This method assumes that all the water upstream will drain to the outlet. Boundaries for watersheds delineated with this method are assumed to be areas of high elevation such as ridges. After the fill layer is created, a flow direction grid is developed using the eight-pour point direction method [9]. The flow direction grid is used to delineate the watershed [15].

### 3.2. Algorithm 2: The Cut Method

The Cut Method (CM) uses the watershed delineated from the SFM and compares it to the original DEM, by using the raster calculator tool in ArcMap to subtract the watershed from the DEM [13]. This process will produce a layer that has zeros and negative values. The negative values represent the depressions that were smoothed using the “fill” tool in ArcMap. Negative values are removed

from the original watershed. Watersheds with little internal drainage will not differ from the SFM watershed [13] [14]. Watersheds with substantial internal drainage will have a “swiss cheese” appearance compared to the original SFM watershed as showing in **Figure 2** [13] [14] [15].

### 3.3. Algorithm 2: The Potentially Contributing Source Areas Method

The Potentially Contributing Source Areas Method (PCSAM) uses several additional inputs to the SFM and CM. It also uses a technique to examine directly connected areas of drainage. The details of the original method can be found in the publication by its developers (Richards and Brenner, 2004) [11]. It was updated and improved upon by Macholl *et al.* (2011) [12] and Troolin and Clancy (2015) [14]. The details of the updated PCSAM are described step by step in Miller and Clancy so that a reader can reproduce the method [15]. The summarized salient details of the PCSAM are summarized for the reader’s convenience in the following text.

Like the CM, the PCSAM uses the SFM watershed as an input. It also requires land use raster and a rasterized version of streams and water bodies. Wetlands are identified and isolated in the wetland land cover. A buffer of 100 meters is developed around the wetlands and streams and is used in the algorithm [15].

The PCSAM algorithm assumes that areas that are directly connected upstream of waterways via wetland and are part of the watershed or “source area.” [11] The algorithm also will iteratively calculate upstream slopes from the wetland/stream source areas and add those to the “source area.” Once the gradient towards the source areas changes direction away from the source area, the algorithm is completed, and the watershed boundaries are designated. Most watersheds delineated with this method will look substantially different from the original SFM as shown in **Figure 2**. Research indicates that in areas with internal drainage, this method is more representative of the watershed because it examines land use, water bodies, and local slope [11] [12] [13] [14] [15].

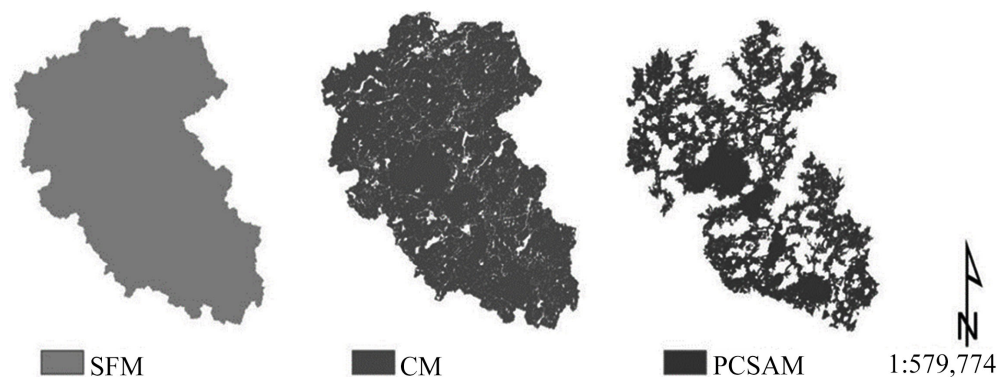


**Figure 2.** Example of the differences in the watershed delineation using the Standard Fill Method (SFM), Cut Method (CM) and the Potential Contributing Source Areas Method (PCSAM) Yahara River at McFarland, WI based on Miller and Clancy (2017) [15].

### 3.4. Runoff Calculations

The National Resource Conservation Service curve number model is an empirical model that parameterizes many of the complexities associated with runoff using two variables: Curve Number ( $CN$ ) and Storage ( $S$ ). The method is extremely popular for quickly assessing runoff impacts and makes several simplifying assumptions. The model assumes that “rainfall excess” occurs when precipitation exceeds the storage capacity or  $S$  of the land [1] [2] [3].  $S$  is determined from empirically derived relationships that account for soil type and land cover.  $S$  is calculated as follows:

$$S = 2540/CN - 254 \quad (1)$$

where  $S$  is storage in mm and  $CN$  is an empirical variable that is determined from a lookup table that requires knowing the soil type and land cover of the area. The storage variable  $S$  assumes that all precipitation that is available for runoff can be absorbed into the soil (if pore space is available). Soil type is classified into four categories: A, B, C, and D [1]. The values A-D are a gradient where A represents high infiltration and low runoff potential and D represents low infiltration and high runoff potential. The land cover is based on the land type categories, typically forest, agriculture, wetland, and urban, making up the four major land cover types. The land cover categories do not fall on a continuum like the soil type category, but it is noted that areas with more urban regions are likely to have low storage capacity and high runoff potential, while areas with more forested regions will have higher storage capacity and lower runoff potential.

The combination of land cover/use and soil type result in a  $CN$ , where high  $CN$ s represent higher runoff and lower  $S$ . An example of this would be a forested region with a Hydrologic Soil Type D will have a lower  $S$  than a forested region with soil type A.

After  $S$  is calculated, its value is compared to the storm’s total precipitation ( $P$ ), and the following condition must be met before calculating runoff:

$$P > 0.2 S \quad (2)$$

This ensures that within the model the precipitation threshold was exceeded for runoff to occur. Otherwise the assumption is that the storage provided by the soil is large enough to store the precipitation [1] [2] [3]. If this assumption is satisfied, then runoff is assumed to occur and is calculated as follows:

$$R = (P - 0.2 S)^2 / (P + 0.8 S) \quad (3)$$

where  $P$  is total precipitation (mm),  $S$  is storage (mm) and  $R$  is runoff (mm). For each grid a land cover and soil type can be determined, a corresponding storage and runoff grid can be calculated for different precipitation events.

### 3.5. Storm Selection (Precipitation)

As indicated by Equation (2), storm selection requires that the precipitation exceeds storage capacity. To ensure this requirement was met, the minimum curve

number was determined for each watershed. Using the minimum *CN* value and Equations (1) and (3), a minimum precipitation can be solved for by substitution. Once the minimum precipitation data is determined, storms can be selected from NCDC [24]. For each watershed, 10 - 12 storms were selected within the past 20 years (1999-2020). Storms with less than the minimum precipitation were discarded. Storms that occurred between April to October were evaluated. Due to early and late freezing temperatures, storms past October and earlier than April were not considered.

A second consideration in storm selection was ensuring storm independence. Dependent storm events occur in the daily discharge record when a storm occurs close in time to a prior storm event. If the stream hydrograph has not returned to baseflow and another storm event affects the hydrograph, the discharge associated with the second storm is dependent on the first precipitation event as well as the second. This causes an anomalously high discharge value to be paired with a precipitation event. To ensure that only independent storms were chosen, the precipitation daily record was checked to see if there were no precipitation events prior to or after it. The time period before and after varied, but the daily discharge hydrograph was examined to ensure the hydrograph had been at baseflow levels before the event and returned to baseflow levels after the event.

Seasonality of local vegetation and temperatures were considered for segregating the precipitation events into spring, summer, and fall. Precipitation events that occurred in April, May, and June were designated as “spring” events. Usually, the ground has thawed, and young plants are beginning to emerge, but they are not fully grown. In some cases, emergence of certain plants occurs in early June. July and August were designated as “summer” where many crops are at their fullness and some harvesting has begun. September and October were designated as fall. During this time leaves are beginning to fall from deciduous trees and harvest is changing the roughness characteristics of the land cover in agricultural landscapes.

### **3.6. Storm Evaluation (Precipitation and USGS Gaging Station Data)**

For each precipitation event, a corresponding set of daily discharge data from each watershed’s USGS gaging station was obtained [23]. The daily discharge was separated into baseflow and runoff using a 5-day minimum moving average by the USGS’s Hydrograph Separation Program (HYSEP) [29] and the USGS Web Hydrograph Analysis Tool (WHAT) [30].

Observed runoff to correspond to precipitation event was determined by examining the dates after the precipitation event. If runoff occurred after a precipitation event, it would be summed up until flow resumed to baseflow levels. Aggregated runoff was converted from  $\text{m}^3/\text{s}$  by dividing by the watershed area (as determined by the algorithm) in square meters and multiplied by the duration of the event. This produced a runoff value in linear units that is comparable

to the runoff value generated from the curve number model.

### 3.7. Statistics and Evaluation of the CN Model

The observed runoff was compared to the modeled runoff for each of the delineation methods. To compare these observed runoff values from the modeled runoff, the standard error was developed. Recall that each delineation method has different total area and differences in the land cover included. The error statistic was developed in Miller and Clancy, 2016 [15] and is used in this research. The equation is as follows:

$$\text{Standard Error} = (Q_{\text{modeled}} - Q_{\text{observed}})/(\text{SFM Watershed Area}) \quad (4)$$

where  $Q_{\text{modeled}}$  is the curve number model derived discharge in cubic meters per second and  $Q_{\text{observed}}$  is the runoff derived from the gaging station data after the baseflow has been separated from the runoff portion of the total daily discharge (cubic meters per second). The SFM watershed is the standard fill watershed (in square meters) that is left to compare all the watersheds and the three delineation methods.

To evaluate the significant differences in the standard error and storm data, the analysis of variance was determined using the statistical package in Rstudio (version 1.4.17). A level of significance (alpha) of 0.1 was used to evaluate the data. Boxplot graphs were created to display the relationship between data sets.

### 3.8. Major Land Cover

Although watersheds were chosen with diverse land cover, most watersheds had a dominate land cover (>30 percent). For example, many of the watersheds had cover types that were in the 30 - 40 percent range for agriculture and forest. Several watersheds had over ten percent urban land use. Even though ten percent appears comparatively small, research suggests that urban land use of ten percent or more has a substantial impact on runoff [21]. Watersheds with greater than 35 percent forest, 35 percent agriculture, and 10 percent urban were identified and examined to see if this land cover dominance introduced bias.

## 4. Results

### 4.1. The Watersheds and the Delineation Method

The eighteen watersheds used in this study are listed in **Table 1**. The SFM watershed is the input for both the CM and PCSAM. Watershed delineated using the SFM will always be equal or larger than watersheds delineated from the other methods. The CM watersheds are very similar to the PCSAM in size except for watersheds that have substantial internal drainage as indicated by lakes or wetlands. Many of the wetlands have been drained since before the 1900s [22]. CM watersheds that have seventy-five percent of the SFM watershed are Fish, White, Allequash, and Bear. These watersheds are in the northern part of the state, which is relatively untouched by urbanization and drainage and channelization associated agriculture.



**Table 1.** List of the watersheds with the watershed area listed by delineation method for the Standard Fill Method (SFM), Cut Method (CM), and Potential Contributing Source Area Method (PCSAM). The input for both the CM and the PCSA method is the SFM watershed, so watershed delineated using those methods will always equal or smaller than the SFM watershed. The CM is very close in delineation size to the SFM. The PCSAM is substantially smaller than the SFM and CM for several watershed.

USGS Name	Short name	SFM (km)	CM (km)	PCSAM (km)	CM percent	PCSAM percent
Menomonee River at Wauwatosa	Menomonee	321.16	314.68	45.71	0.979823	0.142328
Yellow River at Babcock	Yellow	556.85	554.36	85.7	0.995528	0.153901
La Crosse River at Sparta	La Crosse	421.08	420.51	73.09	0.998646	0.173577
Fox River at Waukesha	Fox	318.05	312.72	58.53	0.983242	0.184028
North Fish Creek near Moquah	Fish	220.41	162.39	64.49	0.736763	0.292591
Kickapoo River at La Farge	KLF	686.45	683.06	247.34	0.995062	0.360318
Kickapoo River at State Highway 33 at Ontario	Ontario	302.95	301.63	120.31	0.995643	0.397128
Prairie River near Merrill	Prairie	604.32	548.09	245.3	0.906953	0.405911
White River near Ashland	White	709.02	526.13	318.83	0.742052	0.449677
Yahara River at McFarland	Yahara	876.36	815.42	450.57	0.930462	0.514138
Allequash Creek at County Highway M near Boulder Junction	Allequash	40.57	31.59	22.26	0.778654	0.548681
Bear River near Manitowish Waters	Bear	225.32	166.36	142.9	0.738328	0.634209
Little Turtle Creek at Carvers Rock Road near Clinton	Clinton	517.48	495.57	358.14	0.95766	0.692085
Spirit River at Spirit Falls	Spirit	224.55	217.3	167.3123	0.967713	0.7451
Baraboo River near Baraboo	Baraboo	1575.09	1545.3	1196.48	0.981087	0.759626
Platte River near Rockville	Platte	367.49	364.87	328.17	0.992871	0.893004
Grant River at Burton	Grant	697.14	692.93	630.04	0.993961	0.90375
Pecatonica River at Darlington	PTD	705.25	700.59	642.58	0.993392	0.911138

The PCSAM watersheds sizes are nearly all less than seventy five percent of the SFM except for Platte, Grant, and PTD. The aforementioned watersheds are in the southwestern part of the state and subject to substantial agricultural modifications such as drainage and channelization. Alternatively, Menomonee, Yellow, Sparta, Fox, and Fish watersheds have PCSAM areas less than one third of the SFM. The aforementioned watersheds are spread across the state with no specific geographic concentration.

#### 4.2. Seasonal Precipitation Statistics

As mentioned in the methods section storm events were divided into spring (April, May, June), Summer (July, August) and Fall (September, October) with the storm count being 71, 65, and 35 respectively (Table 2). Figure 3 shows that the average for the storm events was higher for fall but not significantly different average storm events for spring and summer ( $p > 0.1$ ). Figure 4 shows that the average intensity of the storm events was slightly higher for fall, but again not significantly different from spring and summer ( $p > 0.1$ ). Max intensity was higher for summer and spring (5.5, 5.2 mm/hr, respectively) than fall (3.8 mm/hr), but the variance was not significantly different for fall, spring, and

summer ( $p > 0.1$ ). The average storm intensity for fall was significantly different from spring ( $p = 0.09$ ).

In **Figure 5**, the standard error versus precipitation intensity is presented for each delineation method. The PCSAM is biased towards a negative standard error [14] [15]. This means that the modeled runoff is biased towards calculating a runoff value less than the observed, while the CM and SFM over calculate the modeled runoff. Over ninety percent of the standard error values fall within  $\pm 0.1$ .

**Table 2.** Statistics for the precipitation events for each season. The seasons spring (May and June), summer (July, August) and fall (September, October) were categorized based on vegetative grown in Wisconsin.

Season	Average Storm (mm)	Max Storm (mm)	Min Storm Precipitation (mm)	Mean Intensity (mm/hr)	Max Intensity (mm/hr)	Min Intensity (mm/hr)	Count
Fall	82.2	162.1	54.6	2.0	3.8	0.9	35.0
Spring	72.0	147.3	25.4	1.7	5.5	0.4	71.0
Summer	76.5	162.6	10.7	1.9	5.2	0.4	65.0

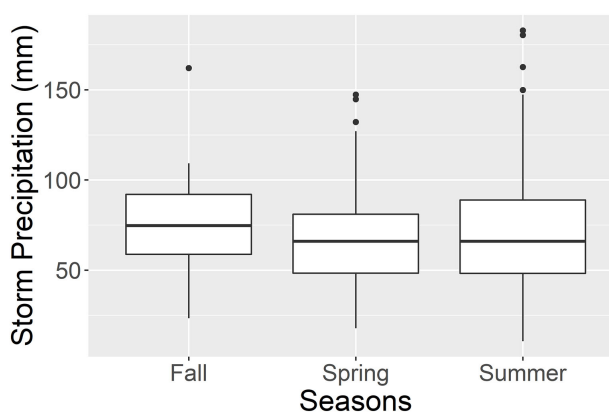


**Figure 3.** No statistically significant difference in the daily precipitation events across the seasons. As mentioned in the text, winter is omitted because of rain on snow events impacting discharge.

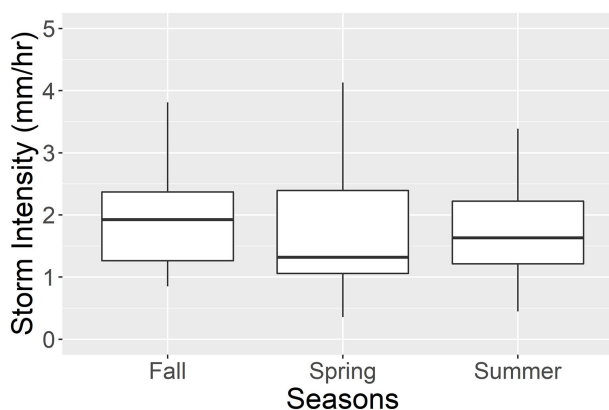


**Figure 4.** Precipitation intensity was not significantly different for the three seasons. Storm intensity is obtained from daily precipitation.

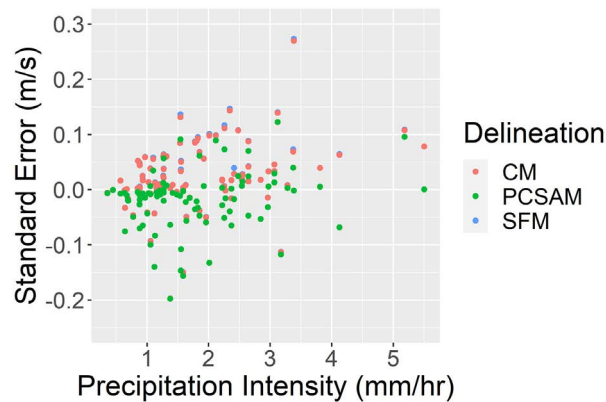


**Figure 5.** For the selected storm events, over 85% of the standard error for precipitation intensity was within  $\pm 0.1$ .

### 4.3. Seasonal Runoff Statistics

In **Table 1**, the runoff error percentage per season for each delineation method is presented. Fall is higher than the other seasons by almost three percent. It is not surprising that overall the errors are lower for the PCSAM delineation compared to the SFM and CM as internal drainage is accounted for in the PCSAM delineation.

The core investigation of this research is presented in **Figures 6-8**. In **Figure 6**, a boxplot graph summarizes the relationship of standard error versus season grouped by delineation. Within the PCSAM watershed, the standard error is not significantly different ( $p > 0.1$ ) for the spring, summer, and fall seasons. The CM and SFM are significantly different from the PCSAM for the fall and summer seasons ( $p < 0.1$ ). Of note is that the CM and SFM within group for spring and summer are significantly different from the fall ( $p < 0.1$ ).

In **Figure 7**, the watersheds with greater than 35 percent forest, 35 percent agriculture, and 10 percent urban were examined and compared in a boxplot graph for each of the seasons and associated standard error for the SFM. Urban watersheds during the summer and agricultural watersheds during the fall have the highest average standard error. Forested land cover was not significantly different ( $p > 0.1$ ) for all three seasons.

In **Figure 8**, the standard error versus delineation type grouped by land use is presented in a boxplot graph. It is expected that the PCSAM will have the lowest standard error compared to the other methods (as shown in **Figure 5**). It is also expected that the CM and SFM have similar standard errors. For all three delineations methods, the forest watersheds have the lowest standard error and are not significantly different than one another. Agriculture land cover has the highest land standard error for the SFM and CM and the lowest standard error for PCSAM. Of interest is that agriculture and urban standard errors are similar for CM and SFM, but the pattern is different for the PCSAM. Forest has a higher absolute value for standard error for PCSAM compared to SFM and CM. Within the PCSAM, the urban appears to be significantly different compared to agriculture.

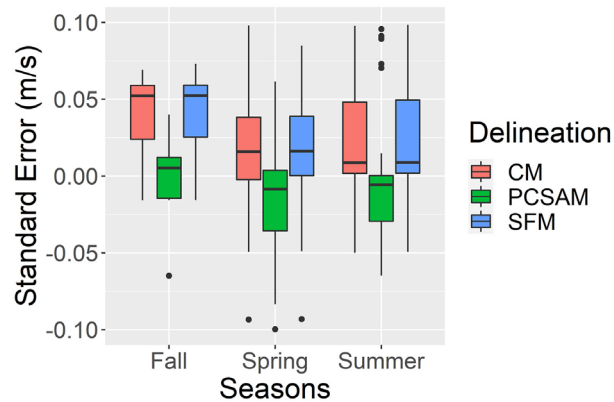


**Figure 6.** PCSAM showed the greatest difference in summer statistically different ( $p < 0.1$ ) and was consistently the same throughout the three seasons examined. Fall and Summer seasons were statistically different for the CM and SFM. Winter was not included due to the rain on snow events that skew observed runoff.

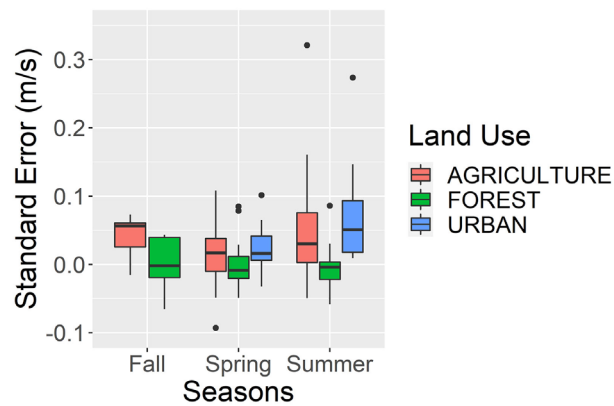


**Figure 7.** Forest land cover was not significantly different ( $p > 0.1$ ) for all three seasons. Urban spring was statistically different from fall and summer ( $p < 0.1$ ). Agricultural fall was statistically different from spring and summer ( $p < 0.1$ ). Winter was not included due to the rain on snow events that skew observed runoff.

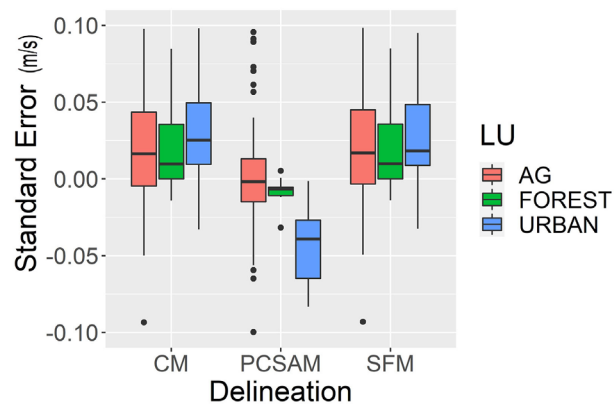


**Figure 8.** For all three delineation types both forest and agriculture are not statistically different ( $p > 0.1$ ) while the PCSAM urban watersheds are statistically different from the SFM and CM ( $p < 0.1$ ). Winter was not included due to the rain on snow events that skew observed runoff.

## 5. Discussion

### 5.1. Precipitation Events

Storm intensities affect runoff. However, storm intensity is not a variable that is considered in curve number in a direct way but rather as a byproduct of the drainage associated with the Hydrologic Soil Group and the storm type [15]. The storms selected for this study are (Figure 4) not statistically significantly different nor providing a hidden impact on the seasons. In Figure 5, the delineation method standard errors generally fall with  $\pm 0.1$ . The standard error does not significantly change with increasing intensity, so storm intensity appears to be an unlikely source of error for this study.

### 5.2. Delineation Methods

The significance of Figure 6 is that the PCSAM method, which considered waterbodies, streams, and wetlands in the delineation, does not change significantly with the seasons. Summer and fall for the SFM and CM are statistically different. Fall has a much higher average (0.28 m) compared to summer average (0.09 m). In fall cases the CM standard error is a little lower than the SFM. The PCSAM method remaining static through the seasons suggests that it is a controlling variable. This finding is also supported by the result in Table 1, where fall has the highest error for the SFM and CM.

### 5.3. Land Use and Seasonality

In Figure 7, the seasons are grouped by major land covers. Spring standard errors are not statistically different from one another, but summer and fall are statistically different. This may suggest that during a cold spring, when vegetation has not emerged, the impact of vegetation is not as pronounced as it is during summer and fall. Also of note is that the largest difference in standard error for the seasons grouped by land cover is between summer and fall agricultural dominant watersheds. This effect is seen in Geng *et al.* (2020) [18] and Hwang *et al.* (2018) [19], where climate had impacted the vegetative type.

The growing season length and average monthly and annual temperatures were not considered in this study. Years with longer growing seasons may distort the standard error. Another consideration may be to examine the earlier spring months (e.g. March and April) and later fall months (October and November) and to include storms from these months in the data. The seasonal impact may be more pronounced using data from a broader seasonal timeline. A future study that considers an extension in the seasonal timeline and growing season is forthcoming using these data.

In Figure 7 the urban land cover is weakly statistically different in spring compared to fall and summer ( $p < 0.1$ ). Urban land cover was aggregated for low, medium, and high intensity development. Generally medium and low intensity urban development has a percentage of land cover allocated to yards and grass. The emergence of grass in spring that is consistently mowed in summer

and fall might account for no seasonal difference in summer and fall.

It is not surprising to see that the CM and SFM watersheds are different from the PCSAM method, but what is interesting about **Figure 8** is that forest dominated watersheds are statistically distinct from urban and agriculture in all delineation methods. Additionally, the relative pattern of the standard error is different for the PCSAM. In the SFM and CM watershed, agriculture and urban standard errors are similar. SFM and CM forest watersheds had the lowest absolute value of standard error. In the PCSAM agricultural dominated watersheds have the lowest absolute value of standard error, followed by forest and then urban. What this observation suggests is that the PCSAM does the best job of modeling agriculture watersheds and forest dominated and urban dominated have a lower standard error. Forest type may also play a role in affecting the standard error. The forests within this study are largely evergreen, so the standard error may be affected differently in watersheds with deciduous forests.

## 6. Conclusion

Observed runoff from a gaging station compared to the CN method for estimating runoff has the highest errors during summer. The CN method shows that the highest runoff overestimates occur in agriculture and urban land covers during summer. Spring months have the lowest standard error. Agricultural land cover standard error is most affected by seasonal differences compared to forest, which has the least seasonal differences in standard error. This study highly suggests that lower curve numbers are required in watersheds dominated by agriculture.

## Acknowledgements

The author wishes to thank Chandra Page for her proofreading expertise and anonymous reviewers who helped with the clarity of this paper.

## Conflicts of Interest

The author declares no conflicts of interest regarding the publication of this paper.

## References

- [1] McCuen, R. (2004) *Hydrologic Analysis and Design*. 3rd Edition, Pearson, Upper Saddle River, 888 p.
- [2] Ponce, V. and Hawkins, R. (1996) Runoff Curve Number: Has It Reached Maturity? *Journal of Hydrologic Engineering*, **1**, 11-19.  
[https://doi.org/10.1061/\(ASCE\)1084-0699\(1996\)1:1\(11\)](https://doi.org/10.1061/(ASCE)1084-0699(1996)1:1(11))
- [3] US Department of Agriculture and Natural Resource Conservation Service (NRCS) (2009) Part 630 Hydrology National Engineering Handbook. Chapter 7, Hydrologic Soil Groups.  
<http://directives.sc.egov.usda.gov/OpenNonWebContent.aspx?content=22526.wba>
- [4] Garen, D.C. and Moore, D.S. (2005) Curve Number Hydrology in Water Quality Modeling: Uses, Abuses, and Future Directions. *Journal of the American Water*

- Resources Association*, **41**, 377-388.  
<https://doi.org/10.1111/j.1752-1688.2005.tb03742.x>
- [5] Lian, H., Yen, H., Huang, J.C., Feng, Q., Qin, L., Bashir, M.A., Wu, S., Zhu, A.X., Luo, J., Di, H., Lei, Q. and Liu, H. (2020) CN-China: Revised Runoff Curve Number by Using Rainfall-Runoff Events Data in China. *Water Research*, **177**, Article ID: 115767. <https://doi.org/10.1016/j.watres.2020.115767>
- [6] Muche, M., Hutchinson, S., Hutchinson, J. and Johnston, J. (2019) Phenology-Adjusted Dynamic Curve Number for Improved Hydrologic Modeling. *Journal of Environmental Management*, **235**, 403-413. <https://doi.org/10.1016/j.jenvman.2018.12.115>
- [7] Karen, G., Patrick, W. and Jos, V. (2021) Performance Evaluation of Spatially Distributed, CN-Based Rainfall-Runoff Model Configurations for Implementation in Spatial Land Use Optimization Analyses. *Journal of Hydrology*, **602**, Article ID: 126872. <https://doi.org/10.1016/j.jhydrol.2021.126872>
- [8] Jenson, S. (1984) Automated Derivation of Hydrological Basin Characteristics from Digital Elevation Data. US Geological Survey Report 14-08-0001-20129, 10 p.  
<http://topotools.cr.usgs.gov/pdfs/automated-derivation-of-hydrologic-basin-characteristics-from-digital-elevation-model-data.pdf>
- [9] Jenson, S. and Domingue, J. (1998) Extracting Topographic Structure from Digital Elevation Data for Geographic Information System Analysis. *Photogrammetric Engineering and Remote Sensing*, **54**, 1593-1600.
- [10] Khan, A., Richards, K., Parker, G., McRobie, A. and Mukhopadhyay, B. (2014) How Large Is the Upper Indus Basin? The Pitfalls of Auto-Delineation Using DEMs. *Journal of Hydrology*, **509**, 442-453. <https://doi.org/10.1016/j.jhydrol.2013.11.028>
- [11] Richards, P. and Brenner, A. (2004) Delineating Source Areas for Runoff in Digresional Landscapes: Implications for Hydrologic Modeling. *Journal of Great Lakes Research*, **30**, 9-21. [https://doi.org/10.1016/S0380-1330\(04\)70325-1](https://doi.org/10.1016/S0380-1330(04)70325-1)
- [12] Macholl, J., Clancy, K. and McGinley, P. (2011) Using a GIS Model to Identify Internally Drained Areas and Runoff Contribution in a Glaciated Watershed. *Journal of the American Water Resources Association*, **47**, 114-125.  
<https://doi.org/10.1111/j.1752-1688.2010.00495.x>
- [13] Troolin, W. (2015) Impacts of Delineation Methods on Modeled Runoff in Watersheds Containing Non-Contributing Internal Drainage. MSc Thesis, University of Wisconsin, Madison.
- [14] Troolin, W. and Clancy, K. (2016) Comparison of Three Delineation Methods Using the Curve Number Method to Model Runoff. *Journal of Water Resources and Protection*, **8**, 945-964. <https://doi.org/10.4236/jwarp.2016.811077>
- [15] Miller, K. and Clancy, K. (2017) Improving Curve Number Runoff Estimates Using Dual Hydrologic Soil Classification and Potential Contributing Source Areas Delineation Methods. *Journal of Water Resources and Protection*, **9**, 20-39.  
<https://doi.org/10.4236/jwarp.2017.91003>
- [16] Peel, M. (2009) Hydrology: Catchment Vegetation and Runoff. *Progress in Physical Geography*, **33**, 837-844. <https://doi.org/10.1177/0309133309350122>
- [17] Descheemaeker, K., Poesen, J., Borselli, L., Nyssen, J., Raes, D., Haile, M., Muys, B. and Deckers, J. (2008) Runoff Curve Numbers for Steep Hillslopes with Natural Vegetation in Semi-Arid Tropical Highlands, Northern Ethiopia. *Hydrological Processes*, **22**, 4097-4105. <https://doi.org/10.1002/hyp.7011>
- [18] Geng, X., Zhou, X., Yin, G., Hao, F., Zhang, X., Hao, Z., Singh, V. and Fu, Y. (2020) Extended Growing Season Reduced River Runoff in Luanhe River Basin. *Journal of Hydrology*, **582**, Article ID: 124538. <https://doi.org/10.1016/j.jhydrol.2019.124538>

- [19] Hwang, T., Martin, K.L., Vose, J.M., Wear, D., Miles, B., Kim, Y. and Band, L.E. (2018) Nonstationary Hydrologic Behavior in Forested Watersheds Is Mediated by Climate-Induced Changes in Growing Season Length and Subsequent Vegetation Growth. *Water Resources Research*, **54**, 5359-5375. <https://doi.org/10.1029/2017WR022279>
- [20] Gal, L., Grippa, M., Hiernaux, P., Pons, L. and Kergoat, L. (2016) The Paradoxical Evolution of Runoff in the Pastoral Sahel: Analysis of the Hydrological Changes over the Agoufou Watershed (Mali) Using the KINEROS-2 Model. *Hydrology and Earth System Sciences*, **21**, 4591-4613. <https://doi.org/10.5194/hess-21-4591-2017>
- [21] Ji, G., Song, H., Wei, H. and Wu, L. (2021) Attribution Analysis of Climate and Anthropogenic Factors on Runoff and Vegetation Changes in the Source Area of the Yangtze River from 1982 to 2016. *Land*, **10**, Article No. 612. <https://doi.org/10.3390/land10060612>
- [22] Homer, C., Dewitz, J., Fry, J., Coan, M., Hossain, N., Larson, C., Herold, N., McKerrow, A., Van Driel, J.N. and Wickham, J. (2007) Completion of the 2001 Land Cover Database for the Conterminous United States. *Photogrammetric Engineering and Remote Sensing*, **73**, 337-341.
- [23] USGS (US Geological Survey) (2021) Geological Survey, National Water Information System: Web Interface, Surface Water for Wisconsin. <http://waterdata.usgs.gov/wi/nwis/rt>
- [24] NCDC (National Climate Data Center) (2020) NCDC Surface Data: Daily. US High Resolution-Cooperative, NWS. <https://www.ncdc.noaa.gov/>
- [25] USGS (US Geological Survey) (2001) NED (National Elevation Data) 2011 Elevation. SDE Raster Digital Data. <http://nationalmap.gov/elevation.html>
- [26] USGS (US Geological Survey) (2011) NLCD (National Land Cover Database) 2011 Land Cover. SDE Raster Digital Data. <https://www.mrlc.gov/>
- [27] Soil Survey Staff, Natural Resources Conservation Service and United States Department of Agriculture (2003) Soil Survey Geographic (SSURGO) Database. <http://sdmdataaccess.nrcs.usda.gov>
- [28] WDNR (Wisconsin Department of Natural Resources) (2007) 24,000 Hydrography Data. Version 6.
- [29] Sloto, R. and Crouse, M. (1996) HYSEP: A Computer Program for Streamflow Hydrograph Separation and Analysis. US Geological Survey Water-Resources Investigations Report.
- [30] Lim, K., Engel, B., Tang, Z., Choi, J., Kim, K., Muthukrishnan, S. and Tripathy, D. (2005) Automated Web GIS Based Hydrograph Analysis Tool, WHAT. *Journal of the American Water Resources Association*, **41**, 1407-1416. <https://doi.org/10.1111/j.1752-1688.2005.tb03808.x>